Transition Metal Chemistry
https://doi.org/10.1007/s11243-018-0201-0

DNA binding, antibacterial and antifungal activities of copper(II) complexes with some S-alkenyl derivatives of thiosalicylic acid

Dušan Lj. Tomović[1] · Andriana M. Bukonjić[1] · Verica V. Jevtić[2] · Zoran R. Ratković[2] · Jovana V. Bogojeski[2] · Ana Đeković[5] · Ivana D. Radojević[3] · Ljiljana R. Čomić[3] · Slađana B. Novaković[4] · Goran A. Bogdanović[4] · Srećko R. Trifunović[2] · Gordana P. Radić[1] · Snežana Cupara[1]

Received: 25 October 2017 / Accepted: 1 January 2018

Abstract

The biological activities of two binuclear copper(II) complexes containing S-alkenyl derivatives of thiosalicylic acid are reported [alkenyl = propenyl (**L1**), isobutenyl (**L2**)]. The structure of the complex with the S-isobutenyl derivative (**C2**) was confirmed by single-crystal X-ray structure analysis, which revealed that the structure consists of centrosymmetric, dinuclear complex molecules [Cu_2(*S*-*i*-butenyl-thiosal)$_4$(DMSO)$_2$] containing two Cu(II) centers bridged by four S-isobutyl-thiosalicylate ligands in a paddle-wheel type structure. The Cu(II) atom is situated in a distorted square-pyramidal environment formed by carboxylate oxygen atoms in the basal plane and a DMSO ligand in the axial position. The reactivities of the complexes toward guanosine-5′-monophosphate (5′-GMP) were investigated. Complex **C2** ([Cu_2(*S*-*i*-butenyl-thiosal)$_4$(H_2O)$_2$]) reacted more rapidly with 5′-GMP than complex **C1**. The interactions of complexes **C1** and **C2** with calf thymus DNA (CT-DNA) were examined by absorption (UV–Vis) and emission spectral studies (ethidium bromide displacement studies), revealing good DNA interaction abilities. The antimicrobial activities of the free ligands and their complexes were tested by microdilution method, and both minimal inhibitory and microbicidal concentrations were determined. All the tested substances demonstrated selective and moderate antibacterial activity on gram-positive bacteria, but low antibacterial activity on gram-negative bacteria. Also, the tested substances demonstrated low antifungal activity.

Electronic supplementary material The online version of this article (https://doi.org/10.1007/s11243-018-0201-0) contains supplementary material, which is available to authorized users.

✉ Gordana P. Radić
vasic_gordana@yahoo.com

✉ Snežana Cupara
snezanacupara@yahoo.com

[1] Department of Pharmacy, Faculty of Medical Sciences, University of Kragujevac, Svetozara Markovića 69, Kragujevac 34000, Republic of Serbia

[2] Department of Chemistry, Faculty of Science, University of Kragujevac, Radoja Domanovića 12, Kragujevac 34000, Republic of Serbia

[3] Department of Biology and Ecology, Faculty of Science, University of Kragujevac, Radoja Domanovića 12, Kragujevac 34000, Republic of Serbia

[4] Laboratory of Theoretical Physics and Condensed Matter Physics, Vinča Institute of Nuclear Sciences, University of Belgrade, PO Box 522, Belgrade 11001, Republic of Serbia

[5] State University of Novi Pazar, Vuka Karadzića bb, Novi Pazar 36300, Republic of Serbia

Introduction

Numerous complexes of transition metals are known to be active biological agents, with a wide range of indications for medical applications [1–4]. In particular, complexes of copper(II) can have remarkable potential for the expression of antimicrobial, antiviral, anti-inflammatory and cytotoxic activity [1–3, 5, 6]. Thiosalicylic acid and its derivatives have a variety of applications, from the treatment of inflammatory, allergic and respiratory diseases [7] to potential applications in the prevention of cirrhosis of the liver [8] and in investigation of the contact sensitivity of drugs [9]. Derivatives of thiosalicylic acid can also be coordinated with many transition metal ions [10, 11]. Esters of thiosalicylic acid may also be used as effective ligands for metal complexation [12–14].

Complexes of copper(II) with a five-membered aromatic heterocyclic ligand proved to be capable of bacterial growth inhibition against *Staphylococcus aureus* and *Escherichia coli* [15]. The complexes of modified ligands with different heterocyclic Schiff bases showed a broad spectrum of

Published online: 23 January 2018

antibacterial (*Escherichia coli, Pseudomonas aeruginosa, Salmonella typhi* and *Staphylococcus aureus*) and antifungal (*Candida albicans, Aspergillus flavus, Aspergillus niger* and *Cladosporium*) activities [16, 17]. Also, copper(II) complexes of some antibiotics (such as ofloxacin and norfloxacin) have been obtained, which is a good approach to the development of antibiotics with reduced levels of resistance [18]. A new concept in improving the bactericidal effect of copper(II) complexes involves selection of ligands based on the lipophilicity of the resulting complex. Increasing lipophilicity enhances the penetration of the complex through the bacterial membranes [19]. The antimicrobial activity of dinuclear and mononuclear copper(II) complexes with substituted carboxylate ligands against bacteria, yeasts and molds has been demonstrated [13, 19–29].

In this paper, we report on the biological activities of previously synthesized S-alkenyl derivatives of thiosalicylic acid and their corresponding copper(II) complexes [30, 31]. The in vitro antibacterial and antifungal screening of the two proligands, S-alkenyl derivatives of thiosalicylic acid [alkenyl = propenyl (**L1**) and isobutenyl (**L2**)], and their corresponding copper(II) complexes (**C1** and **C2**) is described. We have also investigated the interactions of the complexes with guanosine-5′-monophosphate (Scheme 1) and with CT-DNA. The X-ray crystal structure of complex **C2** is also presented.

Experimental

Materials and measurements

All reagents were obtained commercially and used without further purification. Elemental analyses were performed on

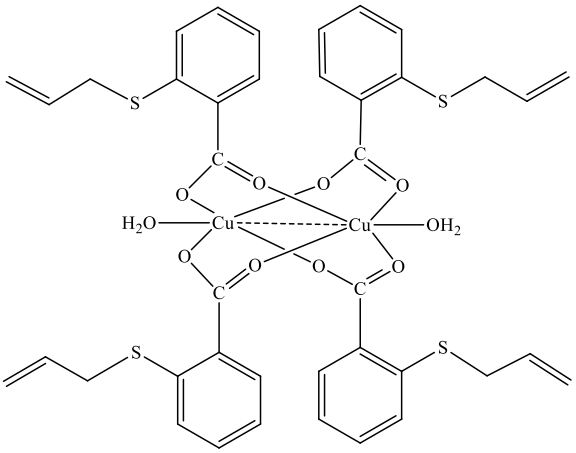

C1

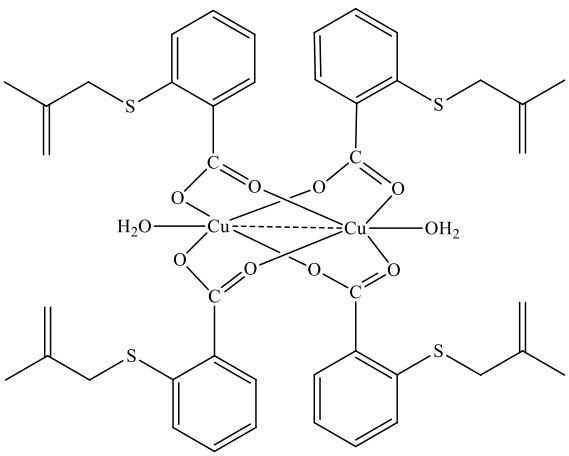

C2

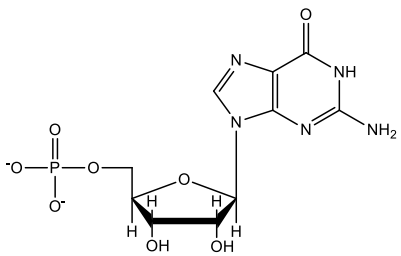

5'-GMP

Scheme 1 Structures of the Cu(II) complexes and 5′-GMP

a Vario III C, H, N, S Elemental Analyzer in CHS mode. Infrared spectra were recorded on a PerkinElmer FTIR 31725-X spectrophotometer using KBr pellets. Conductivity measurements were made at room temperature on freshly prepared 10^{-3} M DMSO solutions using a coronation digital conductivity meter. Kinetics and mechanism of substitution reactions of the complexes with selected ligands were studied in a stopped-flow spectrophotometer in 25 mM Hepes buffer, pH ≈ 7.2 (Acros Organics, Belgium).

Syntheses

The S-alkenyl derivatives of the thiosalicylic acid [alkenyl = propenyl (**L1**), isobutenyl (**L2**)] were prepared [30, 31] by reaction of thiosalicylic acid with the corresponding alkenyl halides in aqueous alkali ethanol solution.

Synthesis of the complexes

Copper(II) nitrate trihydrate (0.1000 g, 0.4139 mmol) was dissolved in water (10.0 mL) on a steam bath, and the required S-alkenyl thiosalicylate [alkenyl = propenyl (**L1**)—0.1607 g, 0.8278 mmol; isobutenyl (**L2**)—0.1724 g, 0.8278 mmol] was added. The mixture was heated for 3 h, during which a solution of LiOH (0.0199 g, 0.8278 mmol) in water (10.0 mL) was added in small portions. The solution was then filtered and evaporated to small volume. The blue precipitate was separated by filtration, washed with cold water and air-dried [30, 31]. In order to obtain single crystals of $[Cu_2(S\text{-isobutenyl-thiosal})_4(H_2O)_2]$ (**C2**) suitable for X-ray diffraction, the complex was recrystallized from H_2O/DMSO mixture.

Complex **C1** $[Cu_2(S\text{-propenyl-thiosal})_4(H_2O)_2]$ = $Cu_2C_{41}H_{43}O_{10}S_4$ (Mr = 951.126): Calcd.: C, 51.77; H, 4.56; S, 13.49. Found: C, 51.54; H, 4.42; S, 13.29%. μ(294 K) = 1.84 μ_B. Molar conductivity 5.06 μS/cm (48s). IR (KBr, cm^{-1}): 3441s, 3076s, 2918m, 1610s, 1549s, 1460m, 1435m, 1400s, 1281w, 1258w, 1229w, 1156w, 1062m, 1044w, 846w, 744m, 695w, 658w, 556w.

Complex **C2** $[Cu_2(S\text{-isobutenyl-thiosal})_4(H_2O)_2]$ = $Cu_2C_{45}H_{51}O_{10}S_4$ (Mr = 1007.232): Calcd.: C, 53.66; H, 5.10; S, 12.73. Found: C, 53.47; H, 5.18; S, 12.64%. μ(294 K) = 1.86 μ_B. Molar conductivity 9.43 μS/cm (48s) IR (KBr, cm^{-1}): 3446s, 2969s, 2915m, 1613s, 1589s, 1400s, 1281w, 1257w, 1157w, 1062m, 847w, 744m, 719w, 656w, 510w [31].

Single-crystal X-ray crystallography

Single-crystal diffraction data for complex **C2** were collected at room temperature on an Oxford Diffraction Gemini S diffractometer equipped with a Mo Kα radiation source and CCD detector. Data reduction and empirical absorption corrections were performed with CrysAlisPro [32]. The structure was solved by direct methods, using SIR2002 [33], and refined using the SHELXL program [34]. The hydrogen atoms attached to C atoms were placed at geometrically idealized positions with C–H distances fixed at 0.93 from Csp^2 and 0.97 and 0.96 Å from methylene and methyl Csp^3, respectively. The isotropic displacement parameters were set at $1.2U_{eq}$ and $1.5U_{eq}$ of the parent C atoms. The DMSO ligand was found to be disordered over two positions, with site occupation factors of 0.80 and 0.20. The treatment of the S atom led to a considerable improvement in the crystal structure model, while the displacement parameters of the disordered C atoms were restrained to isotropic parameters due to instability of the further refinement. All attempts to model the disorder of the S-isobutenyl substituents of the thiosalicylate ligands were unsuccessful. The crystallographic data are listed in Table 1. The PARST [35] and PLATON [36] programs were used to perform geometrical calculations, and the program Mercury [37] was employed for molecular graphics.

Table 1 Crystallographic data for **C2**

Empirical formula	$C_{48}H_{56}O_{10}Cu_2S_6$
Formula weight	1112.4
Color, crystal shape	Green, prism
Crystal size (mm)	0.322 × 0.270 × 0.120
Temperature (K)	293(2)
Wavelength (Å)	0.71,073
Crystal system	Monoclinic
Space group	$P2_1/n$
Unit cell dimensions	
a (Å)	10.8516(4)
b (Å)	10.2909(2)
c (Å)	24.7049(8)
β (°)	100.417(3)
V (Å^3)	2713.4(2)
Z	2
D_{calc} (Mg/m^3)	1.366
μ (mm^{-1})	1.066
θ range for data collection (°)	2.59–28.94
Reflections collected	12,000
Independent reflections, R_{int}	6152, 0.0232
Completeness (%) to $\theta = 26°$	99.9
Refinement method	Full-matrix least squares on F^2
Data/parameters	4576/308
Goodness of fit on F^2	1.021
Final R_1/wR_2 indices [$I > 2\sigma(I)$]	0.0486/0.1257

Kinetic measurements

The substitution reactions of complexes **C1** and **C2** with the nucleophile 5′-GMP were studied spectrophotometrically. Spectral changes resulting from the mixing of the complex and nucleophile solutions were recorded over the wavelength range from 200 to 400 nm in order to establish a suitable wavelength at which kinetic measurements could be performed.

Substitution reactions were initiated by mixing equal volumes of complex and ligand solutions directly in the stopped-flow instrument and followed for at least eight half-lives. The substitution reaction was monitored by the change in absorbance with time under *pseudo*-first-order conditions. The observed *pseudo*-first-order rate constants, k_{obs}, were calculated as the average values from four to six independent kinetic runs using the program OriginPro 8. Experimental data are presented in Tables S1 and S2.

UV–Vis DNA interactions

A stock solution of CT-DNA was prepared in PBS buffer, giving a ratio of UV absorbances at 260 and 280 nm (A_{260}/A_{280}) of ca. 1.8–1.9, indicating that the DNA was sufficiently free of protein. The concentration was determined from the UV absorbance at 260 nm ($\varepsilon = 6600\ M^{-1}\ cm^{-1}$) [38]. The UV–Vis spectra were obtained on a PerkinElmer Lambda 35 or 25 double-beam spectrophotometer, using 1.0 cm path length quartz cuvettes (3.0 mL). Fluorescence measurements were made on an RF-1501 PC spectrofluorometer (Shimadzu, Japan). The fluorescence spectra were recorded in the range 550–750 nm upon excitation at 527 nm in all cases. The excitation and emission bandwidths were both 10 nm.

UV–Vis absorption studies

In order to quantitatively compare the binding strength of the complexes, the intrinsic binding constants K_b were determined by monitoring the changes in absorption of the MLCT band with increasing concentration of CT-DNA, using Eq. (1).

$$[DNA]/(\varepsilon_A - \varepsilon_f) = [DNA]/(\varepsilon_b - \varepsilon_f) + 1/[K_b(\varepsilon_b - \varepsilon_f)] \quad (1)$$

where K_b is given by the ratio of slope to the y intercept in plots of $[DNA]/(\varepsilon_A - \varepsilon_f)$ versus [DNA], [DNA] is the concentration of DNA in base pairs, $\varepsilon_A = A_{obs}/[complex]$, ε_f is the extinction coefficient for the unbound complex and ε_b is the extinction coefficient for the complex in the fully bound form.

Ethidium bromide displacement studies

The relative binding of the complexes to CT-DNA was determined by calculating the quenching constant (K_{sv}) from the slopes of straight lines obtained from Stern–Volmer Eq. (2).

$$I_0/I = 1 + K_{sv}[Q] \quad (2)$$

where I_0 and I are the emission intensities in the absence and the presence of the quencher (complex **C1** or **C2**), respectively, $[Q]$ is the total concentration of quencher and K_{sv} is the Stern–Volmer quenching constant which can be obtained from the slope of the plot of I_0/I versus $[Q]$.

Viscosity measurements

The viscosities of DNA solutions were measured in the presence of increasing amounts of complexes **C1** and **C2**. The flow time was measured with a digital stopwatch. Each sample was measured three times, and the average flow time was calculated. The data were analyzed as $(\eta/\eta_0)^{1/3}$ against r, where η is the viscosity of DNA in the presence of the complex and η_0 is the viscosity of DNA alone in the buffer solution. The viscosities were calculated from the observed flow time of the DNA-containing solutions (t) corrected for the flow time of the buffer alone (t_0), $\eta = (t - t_0)/t_0$.

In vitro antimicrobial assays

The test compounds were dissolved in DMSO and then diluted with nutrient liquid medium to achieve a concentration of 10%. DMSO was purchased from Acros Organics. Resazurin was obtained from Alfa Aesar. Doxycycline (Galenika A.D., Belgrade) was dissolved in Mueller–Hinton broth (Torlak, Belgrade), while antimycotics, fluconazole (Pfizer Inc.) and ketoconazole (Sigma-Aldrich) were dissolved in Sabouraud dextrose broth (Torlak).

The antimicrobial activities were assessed against 18 microorganisms. These included six strains of pathogenic bacteria, including four standard strains (*Escherichia coli* ATCC 25922, *Pseudomonas aeruginosa* ATCC 27853, *Proteus mirabilis* ATCC 12453 and *Staphylococcus aureus* ATCC 25923), plus two clinical isolates (*Bacillus cereus and Salmonella enterica*). Three species of probiotic bacteria (*Bifidobacterium animalis* subsp. *lactis* PMFKGP33, *Lactobacillus plantarum* PMFKG-P31 and *Bacillus subtilis* IP 5832 PMFKG-P32), seven mold species (*Aspergillus niger* ATCC 16404, *Aspergillus flavus* ATCC 9170, *Aspergillus fumigatus* ATTC 204305, *Trichoderma viridae* ATCC 13233, *Penicillium chrysogenum, Penicillium italicum* and *Penicillium expansum*) and two yeast species (*Candida albicans* ATCC 10231 and *Saccharomyces boulardii* PMFKGP34) were also tested. The clinical isolates were

a generous gift from the Institute of Public Health, Kragujevac. The other microorganisms were provided from the collection held by the Laboratory of Microbiology Faculty of Science, University of Kragujevac.

The bacterial suspensions were prepared by the direct colony method. The turbidity of the initial suspension was adjusted using a densitometer (DEN-1, BioSan, Latvia). When adjusted to the turbidity of the 0.5 McFarland's standard [39], the bacterial suspensions contained about 10^8 colony-forming units (CFU)/mL and the yeast suspensions contained 10^6 CFU/mL. Tenfold dilutions of the initial suspension were additionally prepared in sterile 0.85% saline. The suspensions of fungal spores were prepared by gentle stripping of spores from slopes with growing aspergilli. The resulting suspensions were diluted 1:1000 in sterile 0.85% saline.

Antimicrobial activities were tested by determining the minimum inhibitory concentration (MIC) and minimum microbicidal concentration (MMC) using the microdilution plate method with resazurin [40]. The 96-well plates were prepared by dispensing 100 µL of nutrient broth, Mueller–Hinton broth for bacteria and Sabouraud dextrose broth for fungi, into each well. A 100-µL aliquot from the stock solution of the test compound (concentration 2000 µg/mL) was added into the first row of the plate. Then, twofold serial dilutions were performed with a multichannel pipette. The obtained concentration range was from 1000 to 7.8 µg/mL. The method has been described in detail in a previous paper [30].

Doxycycline, fluconazole and ketoconazole were used as positive controls. 10% DMSO (as a solvent control test) was found not to inhibit the growth of the microorganisms. Each test included growth and sterility controls.

All the tests were performed in duplicate, and the MICs were constant. Minimum bactericidal and fungicidal concentrations were determined by plating 10 µL of samples from wells where no indicator color change or no mycelia growth was recorded, onto nutrient agar medium. At the end of the incubation period, the lowest concentration with no growth (no colony) was defined as the minimum microbicidal concentration.

Results and discussion

Synthesis and chemical characterization

S-alkenyl (R = propenyl (**L1**), isobutenyl (**L2**)) derivatives of thiosalicylic acid were prepared [30, 31] by alkylation of thiosalicylic acid with the corresponding alkenyl halogenides in alkaline water–ethanol solution (Scheme 2). The corresponding complexes were obtained by direct reaction of copper(II) nitrate with the S-alkenyl derivatives (molar ratio 1:2) in aqueous solution with satisfactory yields (more than 80%) (Scheme 3). The structure of complex **C2** was determined by X-ray crystallography. In order to obtain single crystals of $[Cu_2(S\text{-isobutenyl-thiosal})_4(H_2O)_2]$ (**C2**) suitable for X-ray diffraction analysis, the complex was recrystallized from H_2O/DMSO solvent mixture. It can be assumed that S-propenyl complex **C1** has the same overall structure as the S-isobutenyl complex **C2**. The molar conductance values of both complexes in DMSO measured at 10^{-3} M concentration are in the range of 5–10 µS/cm, indicating that both complexes behave as non-electrolytes.

The X-ray crystal structure of complex **C2** consists of centrosymmetric, dinuclear complex molecules $[Cu_2(S\text{-isobutenyl-thiosal})_4(DMSO)_2]$ in which two Cu(II) centers are bridged by four S-isobutenyl-thiosalicylate ligands in a paddle-wheel type structure (Fig. 1). Each Cu(II) center is situated in a distorted square-pyramidal environment formed by carboxylate oxygen atoms in the basal plane and a DMSO ligand in the axial position. Selected geometrical parameters for the crystal structure are given in Table 2. The Cu atom is displaced from the square base toward the axial O atom by 0.205(1) Å. The Cu…Cu distance of 2.6430(7) Å is slightly longer in comparison with the value of 2.614 Å found in dimeric copper(II) acetate [41], but closely comparable to those found in polymorphic $[Cu_2(S\text{-propyl-thiosal})_4(DMSO)_2]$, which has values of 2.6407(4) and 2.6398(9) Å in polymorphs I and II, respectively [29].

The coordination bond lengths of the S-isobutenyl-thiosalicylate ligand (Table 2) are within the values

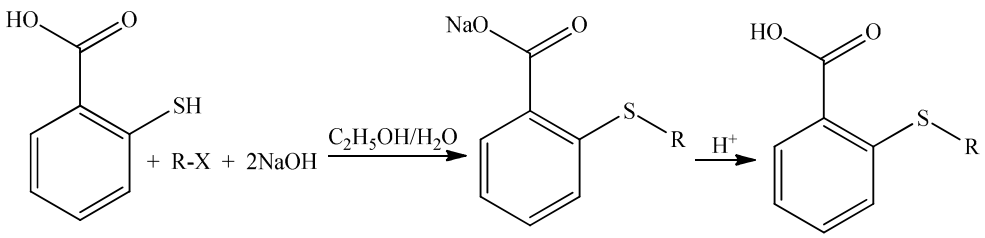

R = propenyl (**L1**), isobutenyl (**L2**)

Scheme 2 Synthesis method of S-alkenyl derivates of thiosalicylic acid

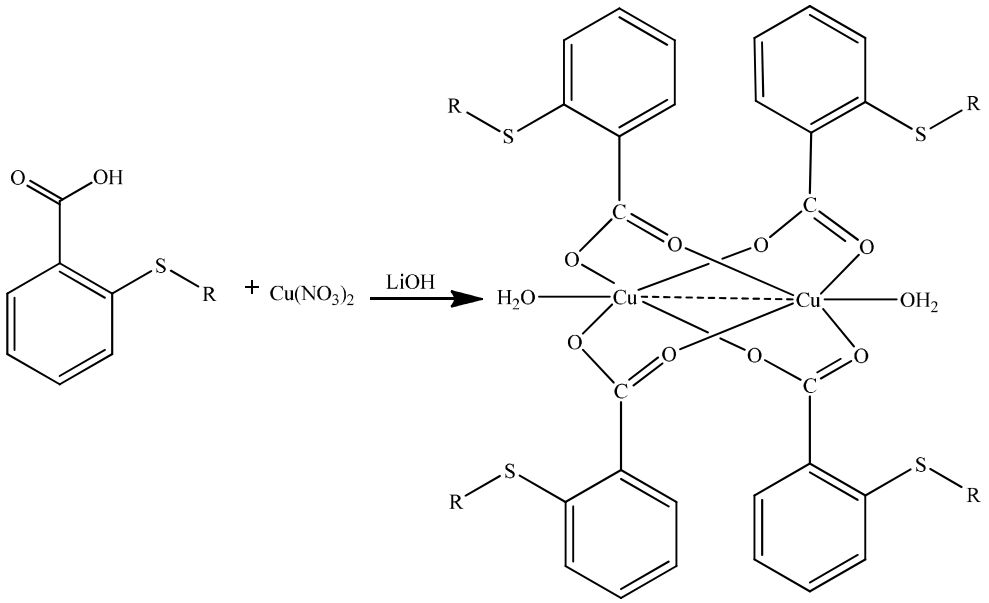

R = propenyl (**C1**), isobutenyl (**C2**)

Scheme 3 Synthesis of copper(II)-complex with S-alkenyl derivates of thiosalicylic acid

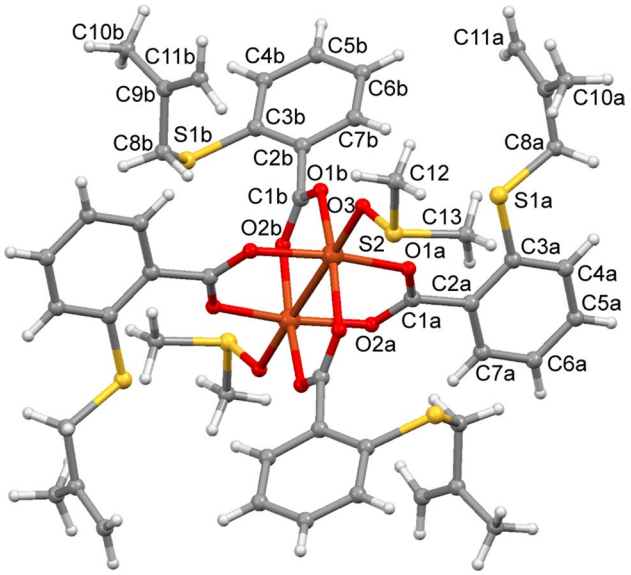

Fig. 1 Crystal structure of $[Cu_2(S\text{-isobutenyl-thiosal})_4(DMSO)_2]$ with the atom-labeling scheme. For the sake of clarity, only the major component of the DMSO ligand is presented

Table 2 Selected bond lengths (Å) and angles (°) of **C2**

Cu1…Cu1^{i}	2.6430(7)	O1a–Cu1–O1b	88.4(1)
Cu1–O1a	1.974(2)	O1a–Cu1–O2b^{i}	89.8(1)
Cu1–O2a	1.968(2)	O1b–Cu1–O2a^{i}	90.0(1)
Cu1–O1b	1.952(2)	O2a^{i}–Cu1–O2b^{i}	89.4(1)
Cu1–O2b	1.967(2)	O1a–Cu1–O3	98.1(1)
Cu1–O3	2.148(2)	O1b–Cu1–O3	98.1(1)
O1a–C1a	1.257(4)	O2a^{i}–Cu1–O3	93.9(1)
O2a–C1a	1.254(4)	O2b^{i}–Cu1–O3	93.9(1)
O1b–C1b	1.256(4)	O1a–Cu1–O2a^{i}	168.1(1)
O2b–C1b	1.256(4)	O1b–Cu1–O2b^{i}	167.98(9)
C3a–S1a	1.762(3)	C1a–C2a–C3a	127.8(3)
C8a–S1a	1.817(5)	O1a–C1a–O2a	125.7(3)
C3b–S1b	1.761(4)	O1b–C1b–O2b	125.6(3)
C8b–S1b	1.799(7)	Cu1^{i}–Cu1–O3	175.17(8)

Symmetry codes: (i) $-x, -y, -z+1$

reported for other complexes of S-propyl derivatives [1.957(4)–1.982(4) Å], as well as those reported for the equivalent Cu(II) complex with the unsubstituted benzoate ligand (1.948–1.985 Å) [42]. In complex **C2** (Fig. 1), ligands A and B show significant conformational differences. The phenyl rings display different rotation about the formally single C1–C2 bonds; hence, the dihedral angles between the mean planes of phenyl C2/C7 and carboxyl groups are 28.0(3) and 52.1(2)° in ligands A and B, respectively (Fig. S1). The maximal dihedral angle of 57.3° for complexes of this type is observed in the S-propyl derivative [29], while in the complex with benzoate ligands [42] the corresponding dihedral angles range from 7.9° to 22.4°. Another conformational difference between the two different ligands of **C2** concerns the S-isobutenyl substituent, which in ligand A prefers an extended form with a C3a–S1a–C8a–C9a torsion angle of −174.4(3)° (Fig. S1). In ligand B, the larger twisting observed for the

phenyl ring is accompanied by pronounced folding of the S-isobutenyl substituent, resulting in a C3b–S1b–C8b–C9b torsion angle of −54.3(5)°. The folding of the S-isobutenyl moiety in ligand B seems to have an important role in arranging the bulky S-isobutenyl substituent next to the S-dimethyl moieties of the axial ligands.

In the crystal packing, weak C–H…π interactions between the neighboring aromatic ligands link the complex molecules into chains extending along the *a* crystallographic axis [C4b–H4b…π^{ii}: C… Cg1 = 3.742(5); H… Cg1 = 2.89 Å; C–H…Cg1 154°; Cg1: centroid of C2a/C7a ring; (ii) = $-x + 1, -y, -z + 1$], as shown in Fig. 2. Taking into account the major orientation of the axial DMSO ligand, one can observe short and directional C–H…O contacts between the axial ligands [C12a–H12c…$O3^{iii}$: H…O 2.47Å, C–H…O 163°; (iii) $-x, -y - 1, -z + 1$] which link the molecular chains along the *b* crystallographic axis (Fig. S2).

Substitution of the complexes with 5′-GMP

To get an idea of the robustness of these complexes in living tissue, the substitution reactions of **C1** and **C2** with a selected nucleophile 5′-GMP, a fragment of DNA (Scheme 1), were investigated. The change in absorbance was followed at suitable wavelengths, as a function of time at 310 K and pH ≈ 7.2. The proposed reaction pathways for all observed substitution processes are presented in Scheme 4. The substitution reactions of both complexes proceeded in two successive reaction steps, both of which were dependent on the nucleophile concentration.

The rate constants for substitution could be determined, under *pseudo*-first-order conditions, from a plot of k_{obs} versus the total nucleophile concentration, according to Eqs. (3) and (4), where Nu = 5′-GMP; the slope of the line represents k_1 or k_2. Plots of $k_{obs1,2}$ versus nucleophile concentration showed a linear dependence with no meaningful intercept for all complexes and substitution steps. The results are summarized in Table 3.

$$k_{obs1} = k_1[Nu] \quad (3)$$

$$k_{obs2} = k_2[Nu] \quad (4)$$

Figure 3 shows the dependence of k_{obs} on nucleophile concentration for complex **C1** (see also Fig. S3).

As expected, the substitution reactions of these complexes were very rapid, as shown in Table 3. Complex **C2** is more reactive toward 5′-GMP than complex **C1**. Since these complexes differ only in the S-alkenyl group, the difference can be attributed to the stronger inductive effect of the isobutenyl group compared to the propenyl group. For both complexes, the second substitution step is significantly slower than the first.

Interactions of the complexes with DNA

The interactions of complexes **C1** and **C2** with CT-DNA were investigated by UV–Vis titrations. The intrinsic equilibrium binding constants (K_b) were evaluated. Complex absorption titration studies were carried out at room temperature using a fixed concentration of the complexes (10 μM) in PBS buffer and varying the amount of CT-DNA (0–15 μM) [43, 44]. Addition of CT-DNA to a solution of either complex resulted in a significant hyperchromic effect with the appearance of a new band at 258 nm, but with only insignificant absorption changes in the region of 300–500 nm; see Figs. 4 and S4. These observations suggest a strong interaction between the complexes and CT-DNA

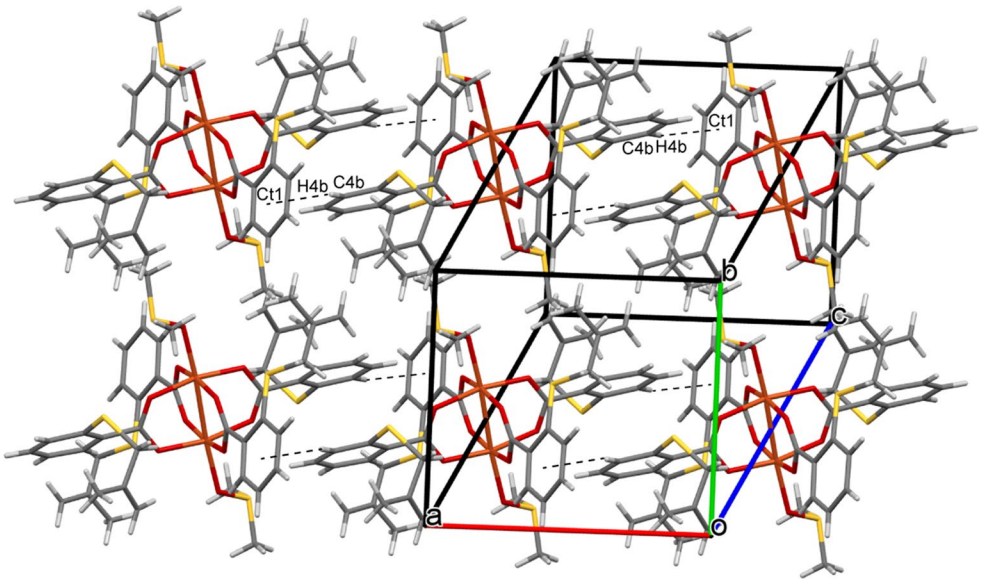

Fig. 2 Crystal packing of complex **C2**. Dashed lines indicate the C–H…π interactions connecting the complex molecules along the *a* axis. For the sake of clarity, only the major component of the DMSO ligand is presented

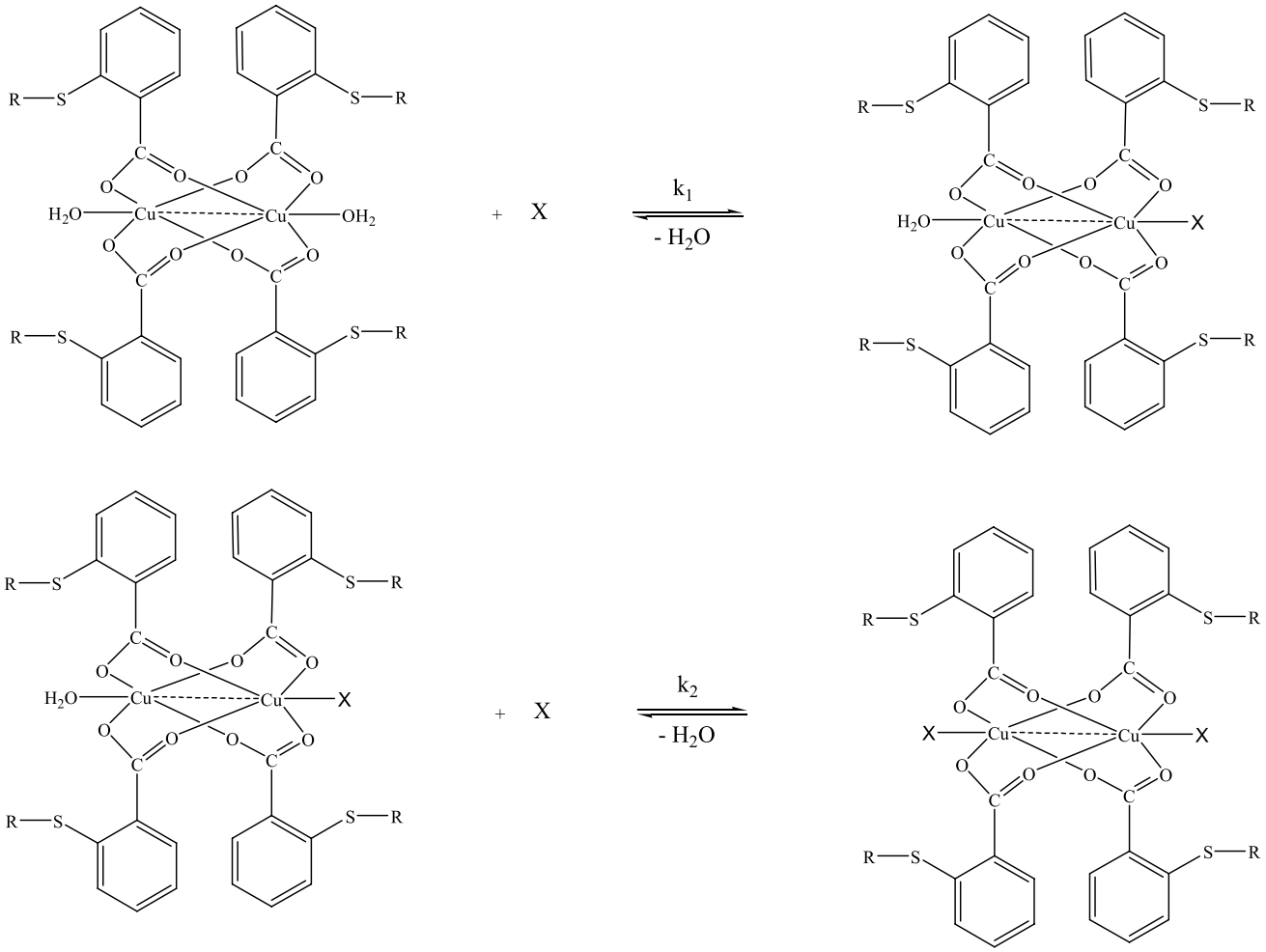

Scheme 4 Substitution reactions of copper(II)-complexes with S-alkenyl derivates of thiosalicylic acid

Table 3 Rate constants for the first and second reaction step of the substitution reactions of the Cu(II)-complexes with 5′-GMP at pH = 7.2 (25 mM Hepes buffer) at 310 K

	5′-GMP	
	First step k_2 [M^{-1} s^{-1}]	Second step k_2 [M^{-1} s^{-1}]
Complex **1**	(6.7 ± 0.2) 10^6	(5.2 ± 0.1) 10^5
Complex **2**	(3.1 ± 0.1) 10^6	(2.3 ± 0.1) 10^5

through external contacts, presumably hydrogen bonding and electrostatic interactions [45, 46].

The interactions of complexes **C1** and **C2** with CT-DNA were also investigated by ethidium bromide (EB) displacement studies. EB fluorescences weakly in free solution [45, 46]; however, in the presence of CT-DNA it strongly emits at ~ 600 nm due to intercalation of EB between DNA base pairs. The addition of either complex **C1** or **C2** to the CT-DNA-EB complex led to significant quenching in fluorescence intensity, due to the displacement of EB. The quenching parameters for the complexes **C1** and **C2** were calculated using the Stern–Volmer equation. Quantitative EB displacement studies were performed by changing the concentrations of the complex and monitoring the emission intensity of the EB-DNA [43, 44]. Increasing concentration of **C1** or **C2** (0–30 μM) resulted in a significant decrease in fluorescence intensity, with a noticeable redshift. Hence, both complexes **C1** and **C2** are capable of displacing EB from the EB-DNA complex and can therefore strongly interact with DNA binding sites (Fig. 5) [47–49].

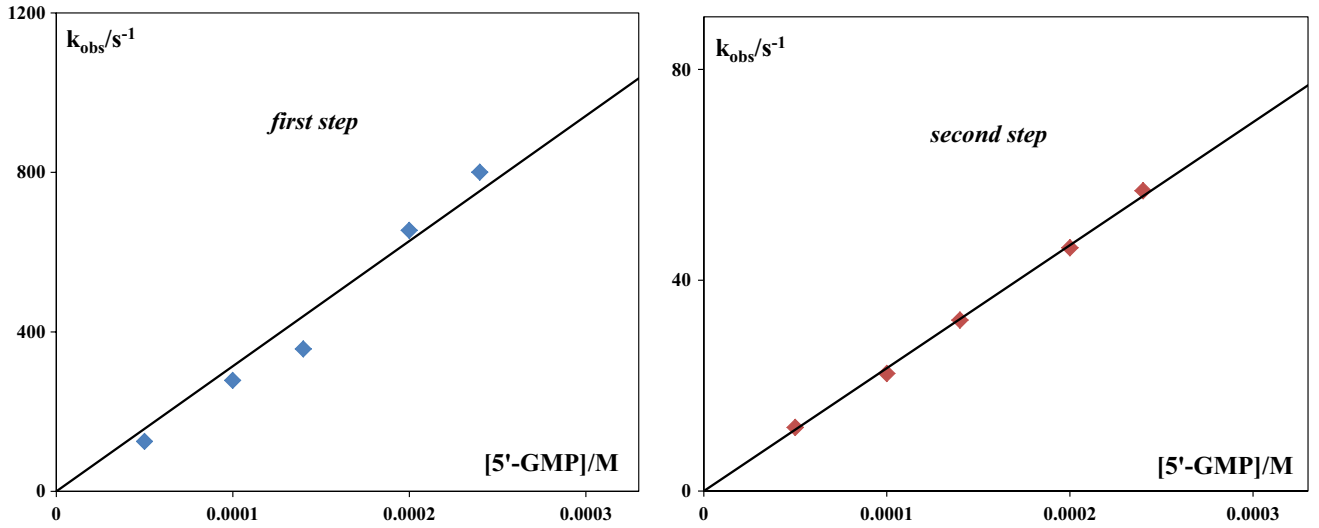

Fig. 3 *Pseudo*-first-order rate constants plotted as a function of nucleophile concentration for the first and second steps of the substitution reactions of complex **C1** with 5′-GMP at pH = 7.2 and 310 K in 25 mM Hepes buffer

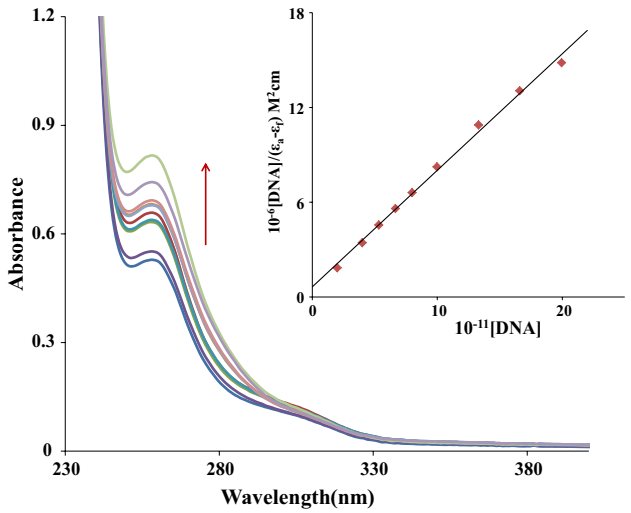

Fig. 4 UV–Vis titration spectra of complex **C1** (10 μM) in PBS buffer (phosphate buffer solution = 0.01 M, C_{NaCl} = 0.137, C_{KCl} = 0.0027 M, pH 7.4) with increasing concentration of CT-DNA (0–15 μM). Arrow shows hyperchromism in the spectral band. Inset: plot of [DNA]/($\varepsilon_A - \varepsilon_f$) versus [DNA]

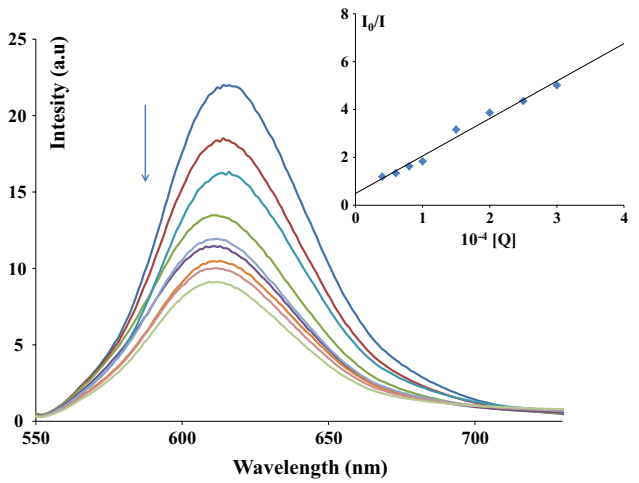

Fig. 5 Fluorescence titration spectra of EB (10 μM) bound to DNA (10 μM) in the presence of varying amounts of complex **C1**. [Arrow shows changes in fluorescence intensity upon increasing concentration of **C1** (4–30 μM)]. Inset: Stern–Volmer plots for EB-DNA fluorescence titration with **C1**

According to the constants presented in Table 4, these complexes interact strongly with CT-DNA, in good agreement with the UV–Vis spectroscopic studies.

In order to further characterize the binding of these complexes to DNA, viscosity measurements of DNA solutions were performed in the presence and absence of the complexes. The viscosity of DNA is sensitive to changes in length, and in the absence of X-ray crystal structure data, this is regarded as the most critical evidence in identifying the DNA binding mode in solution [50, 51]. The addition

Table 4 Obtained constants for interaction between complexes **C1** and **C2** with CT-DNA

	CT-DNA	
	K_b [M^{-1}]	K_{sv} [M^{-1}]
Complex **1**	$(1.3 \pm 0.1) \times 10^6$	$(1.7 \pm 0.1) \times 10^5$
Complex **2**	$(1.1 \pm 0.1) \times 10^6$	$(1.6 \pm 0.1) \times 10^5$

of increasing amounts (up to $r = 1.0$) of complexes **C1** and **C2** to a DNA solution (0.01 mM) resulted in an increase in the relative viscosity of DNA (Fig. S5), which was more pronounced upon the addition of complex **C1**. In the case of classic intercalation, the DNA base pairs are separated to host the bound compound, resulting in an increase in DNA viscosity, the magnitude of which is usually proportional to the strength of the interaction. Hence, the observed viscosity increase for these complexes is another indication of an intercalative interaction with DNA.

Microbiological studies

The results of in vitro testing of antimicrobial activities for both the free ligands and their copper(II) complexes are shown in Table 5. MIC and MMC values, along with those for doxycycline, fluconazole and ketoconazole, are listed in Table 6. All of the test compounds showed moderate and selective antimicrobial activities. MIC and MMC values for the complexes were in range 31.25 to > 1000 µg/mL. The best results were however still lower than the positive control values.

In general, the activities of the complexes were higher than, or similar to the corresponding free ligands. The exception, where the free ligands gave higher activities, are bacteria *Bacillus cereus* (for **L1** and **L2**) and *Salmonella enterica* (for **L2**). Gram-positive bacteria demonstrated slightly higher sensitivities than the gram-negative strains. Among gram-positive bacteria, *Staphylococcus aureus* ATCC 25923 demonstrated the highest resistance (MICs/MMCs are 1000/> 1000 µg/mL). The probiotic bacteria showed the highest sensitivities. The most sensitive was *Bifidobacterium animalis* subsp. *lactis,* with an MIC value of 31.25 µg/mL for complex **C1**. Overall the copper(II) complexes showed low antifungal activities. The test compounds showed little or no effect on the growth of yeasts and other fungi, with MIC and MMC values which were from 250 to > 1000 µg/mL.

In previous work, the Cu(II) complexes of some other S-alkyl derivatives of thiosalicylic acid (alkyl = benzyl; methyl; ethyl; propyl; butyl) were tested against gram-positive and gram-negative bacteria as well as fungi [13, 29]. In general, the activities of the complexes were higher or similar than those of the corresponding free ligands. All the tested complexes demonstrated moderate or selective antibacterial activity and low antifungal activity, which is in accordance with the present results.

Previous research into the antimicrobial activities of dinuclear and mononuclear copper(II) complexes of carboxylate ligands has provided diverse conclusions. Some binuclear Cu(II) carboxylate complexes show no antibacterial activity [20]. The lack of specificity suggests that the sensitivity of various microorganisms to the complexes is not related to the different cell wall structures [20]. There

Table 5 In vitro antimicrobial activity of the ligands **L1** and **L2** and the copper(II)-complexes **C1** and **C2** with positive controls

Species	ML06—L1		MN06—C1		ML07—L2		MN07—C2	
	MIC[a]	MMC[b]	MIC	MMC	MIC	MMC	MIC	MMC
Bifidobacterium animalis subsp. *lactis*	250	500	31.25	500	1000	1000	500	500
Lactobacillus plantarum	500	1000	500	500	1000	1000	500	500
Bacillus subtilis IP 5832	500	1000	500	1000	500	1000	500	500
Bacillus cereus	62.5	250	1000	1000	62.5	250	1000	1000
Staphylococcus aureus ATCC 25923	1000	> 1000	1000	1000	> 1000	> 1000	1000	1000
Pseudomonas aeruginosa ATCC 27853	1000	> 1000	1000	> 1000	> 1000	> 1000	1000	> 1000
Proteus mirabilis ATCC 12453	> 1000	> 1000	1000	> 1000	> 1000	> 1000	500	500
Escherichia coli ATCC 25922	1000	> 1000	1000	> 1000	1000	> 1000	1000	> 1000
Salmonella enterica	500	1000	1000	1000	250	1000	1000	> 1000
Saccharomyces boulardii	500	1000	500	1000	1000	> 1000	500	1000
Candida albicans ATCC 10231	1000	> 1000	1000	1000	1000	> 1000	500	500
Penicillium chrysogenum	250	1000	500	> 1000	500	> 1000	250	1000
Penicillium italicum	1000	1000	250	> 1000	500	> 1000	250	> 1000
Penicillium expansum	1000	1000	> 1000	> 1000	> 1000	> 1000	1000	> 1000
Trichoderma viridae ATCC 13233	1000	1000	1000	1000	1000	1000	500	1000
Aspergillus flavus ATCC 9170	1000	1000	500	1000	1000	1000	500	1000
Aspergillus fumigatus ATTC 204305	1000	1000	1000	1000	1000	1000	1000	1000
Aspergillus niger ATCC 16404	> 1000	> 1000	500	1000	> 1000	> 1000	500	1000

[a]MIC values (µg/mL)—inhibitory activity

[b]MMC values (µg/mL)—microbicidal activity; "/"—not tested

Table 6 In vitro antimicrobial activity of the positive controls (doxycycline for bacteria; fluconazole and ketoconazole for fungi)

Species	Doxycycline		Fluconazole		Ketoconazole	
	MIC[a]	MMC[b]	MIC	MMC	MIC	MMC
Bifidobacterium animalis subsp. *lactis*	31.25	62.50	/	/	/	/
Lactobacillus plantarum	0.45	7.81	/	/	/	/
Bacillus subtilis IP 5832	1.95	15.63	/	/	/	/
Bacillus cereus	0.98	7.81	/	/	/	/
Staphylococcus aureus ATCC 25923	0.22	3.75	/	/	/	/
Pseudomonas aeruginosa ATCC 27853	62.5	125	/	/	/	/
Proteus mirabilis ATCC 12453	15.63	62.5	/	/	/	/
Escherichia coli ATCC 25922	15.63	31.25	/	/	/	/
Salmonella enterica	15.63	31.25	/	/	/	/
Saccharomyces boulardii	/	/	31.25	1000	/	/
Candida albicans ATCC 10231	/	/	31.25	1000	31.25	/
Penicillium chrysogenum	/	/	62.5	500	62.5	/
Penicillium italicum	/	/	1000	1000	125	/
Penicillium expansum	/	/	/	/	62.5	/
Trichoderma viridae ATCC 13233	/	/	/	/	62.5	/
Aspergillus flavus ATCC 9170	/	/	62.50	125	125	/
Aspergillus fumigatus ATTC 204305	/	/	/	/	125	/
Aspergillus niger ATCC 16404	/	/	62.5	62.5	62.5	/

[a]MIC values (μg/mL)—inhibitory activity

[b]MMC values (μg/mL)—microbicidal activity; "/"—not tested

are studies that show good antimicrobial activities of Cu(II) complexes, including activities better than standard drugs [19, 25–27]. Others Cu(II) carboxylate complexes exhibit moderate antibacterial activity [21–28], which is in accordance with our previous [13] and current research. In most studies, as in the present case, weak antifungal activity is observed [22, 23, 25].

Conclusion

In the crystal structure of the dinuclear complex $[Cu_2(S\text{-isobutenyl-thiosal})_4(DMSO)_2]$, the two Cu(II) centers are bridged by four S-isobutenyl-thiosalicylate ligands in a paddle-wheel type structure. The metal atoms are situated in a distorted square-pyramidal environment, provided by oxygen atoms of carboxylate ligands in the basal plane, and a DMSO ligand in the axial position. The order of reactivity of the studied complexes toward 5′-GMP showed that the S-isobutenyl derivative reacted more rapidly than the S-isobutenyl derivative as free ligand. Both of these complexes exhibited strong interactions with DNA. Both the free ligands and their copper(II) complexes demonstrated selective and moderate antibacterial activities against gram-positive bacteria and low antibacterial activities against gram-negative bacteria. Also, the tested substances showed low antifungal activities.

Supplementary data

CCDC 1535567 contains the supplementary crystallographic data for this paper. These data can be obtained free of charge via http://www.ccdc.cam.ac.uk/conts/retrieving.html or from the Cambridge Crystallographic Data Centre, 12 Union Road, Cambridge CB2 1EZ, UK; fax: (+44) 1223 336 033; or e-mail: deposit@ccdc.cam.ac.uk.

Acknowledgements This work was financially supported by the Ministry of Education, Science and Technological Development of the Republic of Serbia (Projects 172016, 173032, 172034, 172035, 172011).

References

1. Tisato F, Marzano C, Porchia M, Pellei M, Santini C (2010) Med Res Rev 30:708–749
2. Marzano C, Pellei M, Tisato F, Santini C (2009) Anticancer Agents Med Chem 9:185–211
3. Prudhomme M (2013) Advances in anticancer agents in medicinal chemistry. Bentham Science Publishers, Clermont-Ferrand

4. Gielen M, Tiekink ER (2005) Metallotherapeutic drugs and metal-based diagnostic agents: the use of metals in medicine. Wiley, Chichester
5. Goodman VL, Brewer GJ, Merajver SD (2004) Endocr Relat Cancer 11:255–263
6. Iakovidis I, Delimaris I, Piperakis SM (2011) Mol Biol Int 2011:1–13
7. H. Jacobelli, US Patent 20050267095
8. Reif S, Weis B, Aeed H et al (1999) J Hepatol 31:1053–1061
9. Serrano G, Bonillo J, Aliaga A et al (1990) J Am Acad Dermatol 23:479–483
10. Ferrer EG, Williams PA (1997) Polyhedron 16:3323–3325
11. Wehr-Candler T, Henderson W (2016) Coord Chem Rev 313:111–155
12. Gilbert JG, Addison AW, Nazarenko AY, Butcher RJ (2001) Inorg Chim Acta 324:123–130
13. Nikolić MV, Mijajlović MŽ, Jevtić VV et al (2014) Polyhedron 79:80–87
14. Nikolić MV, Mijajlović MŽ, Jevtić VV et al (2016) J Mol Struct 1116:264–271
15. Chohan ZH, Shad HA, Youssoufi MH, Hadda TB (2010) Eur J Med Chem 45:2893–2901
16. Patil SA, Naik VH, Kulkarni AD, Badami PS (2010) Spectrochim Acta A Mol Biomol Spectrosc 75:347–354
17. Shebl M, Khalil SM, Ahmed SA, Medien HA (2010) J Mol Struct 980:39
18. Katsarou ME, Efthimiadou EK, Psomas G, Karaliota A, Vourloumis D (2008) J Med Chem 51:470–478
19. Siddiqi ZA, Khalid M, Kumar S, Shahid M, Noor S (2010) Eur J Med Chem 45:264–269
20. Betanzos-Lara S, Gracia-Mora I, Granada-Macyas P, Flores-Alamo M, Barba-Behrens N (2013) Inorg Chim Acta 397:94–100
21. Abou-Hussein AA, Linert W (2012) Spectrochim Acta Part A Mol Biomol Spectrosc 95:596–609
22. Amer S, El-Wakiel N, El-Ghamry H (2013) J Mol Struct 1049:326–335
23. Creaven BS, Egan DA, Karcz D (2007) J Inorg Biochem 101:1108–1119
24. Efthimiadou EK, Katsarou ME, Karaliota A, Psomas G (2008) J Inorg Biochem 102:910–920
25. El-Gamel NE, Zayed MA (2011) Spectrochim Acta Part A 82:414–423
26. Geeta B, Shravankumar K, Muralidhar Reddy P (2010) Spectrochim Acta Part A 77:911–915
27. Siddiqi ZA, Sharma PK, Shahid M, Khalid M, Siddique A, Kumar S (2012) Eur J Med Chem 57:102–111
28. Chalkidou E, Perdih F, Turer I, Kessissoglou PD, Psomas G (2012) J Inorg Biochem 113:55–65
29. Bukonjić AM, Tomović DL, Nikolić MV et al (2017) J Mol Struct 1128:330–337
30. Radić GP, Glođović VV, Radojević ID et al (2012) Polyhedron 31:69–76
31. Tomović DL, Bukonjić AM, Kočović A et al (2017) Serb J Exp Clin Res. 18:13–18
32. Agilent, CrysAlis PRO (2014) PRO. England, Agilent Technologies, Yarnton, Oxfordshire
33. Burla MC, Camalli M, Carrozzini B et al (2003) J Appl Crystallogr 36:1103
34. Sheldrick GM (2008) Acta Crystallogr A 64:112–122
35. Nardelli M (1995) J Appl Crystallogr 28:659
36. Spek AL (2003) J Appl Crystallogr 36:7–13
37. Macrae CF, Edgington PR, McCabe P et al (2006) J Appl Crystallogr 39:453–457
38. Meadows KA, Liu F, Sou J, Hudson BP, McMillin DR (1993) Inorg Chem 32:2919–2923
39. Andrews JM (2005) J Antimicrob Chemoth 56:60–76
40. Sarker SD, Nahar L, Kumarasamy Y (2007) Methods 42:321–324
41. Van Niekerk JN, Schoening FR (1953) Acta Crystallogr 6:227–232
42. Reyes-Ortega Y, Alcantara-Flores JL, Hernandez-Galindo MC (2005) J Am Chem Soc 127:16312–16317
43. Long EC, Barton JK (1990) Acc Chem Res 23:271–273
44. Pasternack RF, Gibbs EJ, Villafranca JJ (1983) J Biochem 22:251
45. Koumousi ES, Zampakou M, Raptopoulou CP et al (2012) Inorg Chem 51:7699–7710
46. Rizvi MA, Zaki M, Afzal M et al (2015) Eur J Med Chem 90:876–888
47. Meyer-Almes FJ, Porschke D (1993) Biochemistry 32:4246–4253
48. Liu ZC, Wang BD, Yang ZY, Li Y, Qin DD, Li TR (2009) Eur J Med Chem 44:4477–4484
49. Howe GM, Wu KC, Bauer WR (1976) Biochemistry 19:4339–4346
50. Li DD, Tian JL, Gu W, Liu X, Yan SP (2010) J Inorg Biochem 104:171–179
51. Jiang M, Li Y, Wu Z, Liu Z, Yan C (2009) J Inorg Biochem 103:833–844